ELSEVIER

Polymer 44 (2003) 1045–1049

polymer

www.elsevier.com/locate/polymer

Cold crystallization of poly(ethylene naphthalene-2,6-dicarboxylate) by simultaneous measurements of X-ray scattering and dielectric spectroscopy

I. Šics[a], T.A. Ezquerra[b,*], A. Nogales[c], Z. Denchev[d], C. Alvarez[b], S.S. Funari[e]

[a]*Institute of Polymer Materials, Riga Technical University, 4 Azenes str., Riga, LV 1048, Latvia*
[b]*Instituto de Estructura de la Materia, C.S.I.C. Serrano 119, Madrid 28006, Spain*
[c]*JJ Thomson Laboratory, The University of Reading, Whiteknights RG6 6AF, UK*
[d]*Department of Polymer Engineering, University of Minho, Guimarães 4800-038, Portugal*
[e]*Max-Planck Intitute for Colloids and Surfaces, c/o HASYLAB, DESY, Notkestraße 85, 22603 Hamburg, Germany*

Received 19 June 2002; received in revised form 10 September 2002; accepted 10 October 2002

Abstract

The isothermal cold crystallization of poly(ethylene naphthalene-2,6-dicarboxylate) was investigated by simultaneous small and wide angle X-ray scattering and dielectric spectroscopy (DS). By this experimental approach, simultaneously collected information was obtained about the specific changes occurring in both crystalline and amorphous phases during crystallization, namely about the chain ordering through wide angle X-ray scattering, about the lamellar crystals arrangement by means of small angle X-ray scattering, and about the amorphous phase evolution by means of DS. The results indicate that average mobility of the amorphous phase suffers a discontinuous decrease upon passing from the primary to the secondary crystallization regime. We interpret these results assuming that the restriction to the mobility of the amorphous phase occurs mainly in the amorphous regions between the lamellar stacks and not in the amorphous regions within the lamellar stacks.

Keywords: Polymer crystallization; Real time; Dielectric spectroscopy

1. Introduction

It is known that some glass forming polymers may develop a semicrystalline state characterised by a folded lamellar morphology at the nanometer level when they are heated from the glassy state above the glass transition temperature, T_g. This process is frequently referred to as 'cold crystallization'. In general, information about the structure of the ordered regions in polymers at different length scales can be obtained by means of X-ray scattering techniques [1,2]. Wide angle X-ray scattering (WAXS) offers the possibility to obtain information about molecular ordering in the scale of tenths of nanometers. On the other hand, small angle X-ray scattering (SAXS) allows one to analyse the structure developed over the length scale of tens of nanometers. Synchrotron radiation offers a further possibility to perform real time, simultaneous SAXS and WAXS experiments during crystallization [3], thus enhancing the understanding of the correlation between nanostructure and crystal development. By using simultaneously both techniques, the ordering of the macromolecules through a very broad length scale can be examined. X-ray scattering techniques can also be used to obtain structural information in amorphous materials [4]. However, in semicrystalline systems mainly information about the ordered regions is obtained due to the fact that the ordered regions provoke strong diffraction phenomena superimposed over a relatively weak contribution of the amorphous phase. As far as the amorphous phase is concerned, dielectric spectroscopy experiments (DS) have shown that, upon crystallization, the amorphous phase segmental dynamics is strongly affected by the progressive development of the crystalline phase [5–8]. Hence, if one could monitor the microstructure development, by X-ray scattering methods, and the dynamic changes occurring in the amorphous phase, by dielectric relaxation methods, a more complete picture of the crystallization process could

* Corresponding author.
E-mail address: imte155@iem.cfmac.csic.es (T.A. Ezquerra).

0032-3861/03/$ - see front matter
PII: S0032-3861(02)00742-5

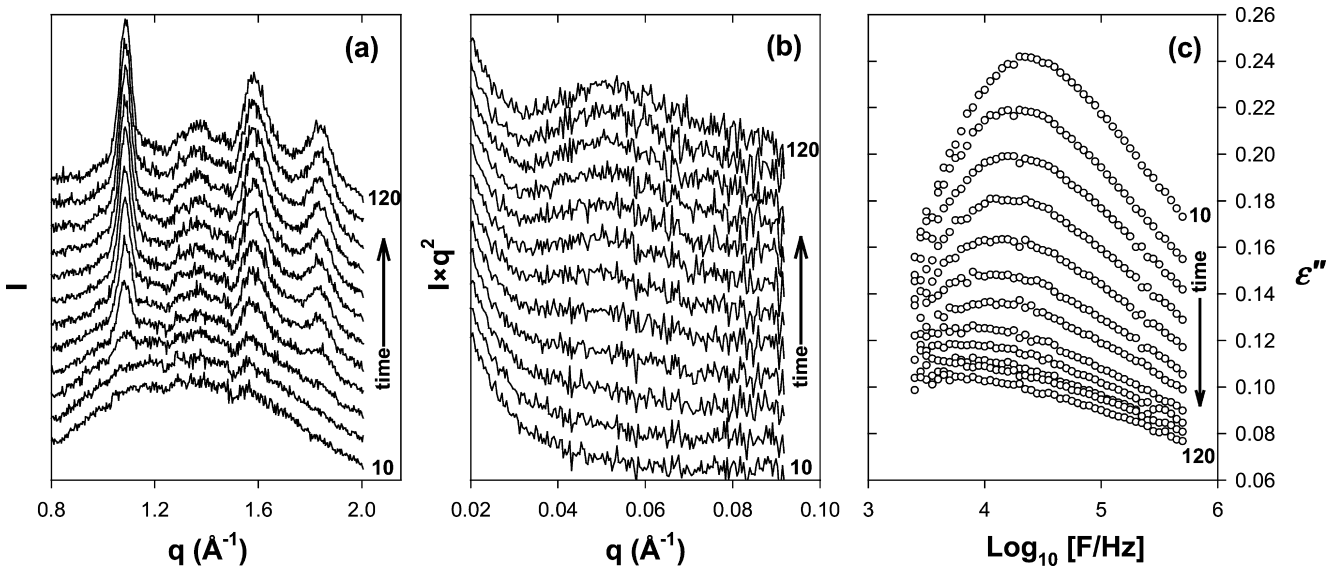

Fig. 1. Simultaneous WAXS (a), SAXS (b) and Dielectric loss, ε'' (c) experiment during crystallization of initially amorphous PEN at $T_c = 152$ °C. The different patterns are shown at 10 min intervals. The X-ray patterns are vertically shifted for the sake of clarity.

be obtained. This experimental procedure has been used to probe cold crystallization of different polyesters [9,10].

Poly(ethylene naphthalene 2,6-dicarboxylate) (PEN) has a chemical structure very similar to that of PET. In its main chain, PEN contains naphthalene rings thus forming a structure being stiffer than that of PET [11–13]. Therefore, as compared to PET, glassy PEN displays a higher glass transition temperature, enhanced mechanical properties like tensile modulus, creep resistance and hardness, as well as a lower shrinkage and better barrier properties [12,13]. Because of these reasons, PEN is gaining increasing importance as a commercial engineering material.

The objective of this contribution is to show that, an improvement in the understanding of the cold crystallization process in PEN can be obtained if the SAXS and WAXS experiments are accompanied by DS, all the three techniques being performed simultaneously (SWD) [14]. It will be shown that in a SWD crystallization experiment one may monitor simultaneously and in real time both the microstructure development (through SAXS and WAXS), and the dynamic changes occurring in the amorphous phase during the development of lamellar structure (by means of DS).

2. Experimental

2.1. Sample description

Amorphous films of 0.2 mm thickness were produced by compression moulding of PEN granulate (Eastman, $M_v \approx 25000$ g/mol) at 300 °C for 3 min and subsequent quenching in ice water. Prior to the hot pressing, the original pellets were dried under vacuum for a given time to eliminate any existing traces of humidity that could cause hydrolysis during the preparation or investigation of the samples.

2.2. Techniques

The simultaneous SAXS–WAXS–DS experiments were performed in the Soft Condensed Matter beam-line A2 at HASYLAB (DESY) synchrotron facility in Hamburg (Germany). To enable simultaneous measurements of SAXS and WAXS, as well as of DS in real time, a recently developed experimental cell (denominated as SWD) was employed [9,10,14]. A detailed description has been reported elsewhere [14]. The SWD cell was incorporated to a vacuum chamber (10^{-2} Torr) specially designed to perform X-ray scattering measurements with synchrotron radiation. A wavelength $\lambda = 0.15$ nm was employed for X-ray diffraction study. A semicrystalline PET standard sample was used for the WAXS and rat tendon tail for the SAXS calibration. Each frame was collected during 60 s and later corrected for primary beam intensity fluctuations during experiment and background. Complex dielectric permittivity measurements, ($\varepsilon^* = \varepsilon' - i\varepsilon''$) were performed in the frequency range of $10^3 < F < 10^6$ Hz, using a Hewlett-Packard 4192 impedance analyser. Circular electrodes, 3 cm diameter, were employed to prepare a sandwich type capacitor and introduced in an on-purpose designed cell described elsewhere [14].

3. Results

Fig. 1 shows the simultaneously obtained SWD data collected during a crystallization experiment at $T_c = 152$ °C for different crystallization times. Both, WAXS and Lorentz corrected SAXS intensities [1] are given as a function of the

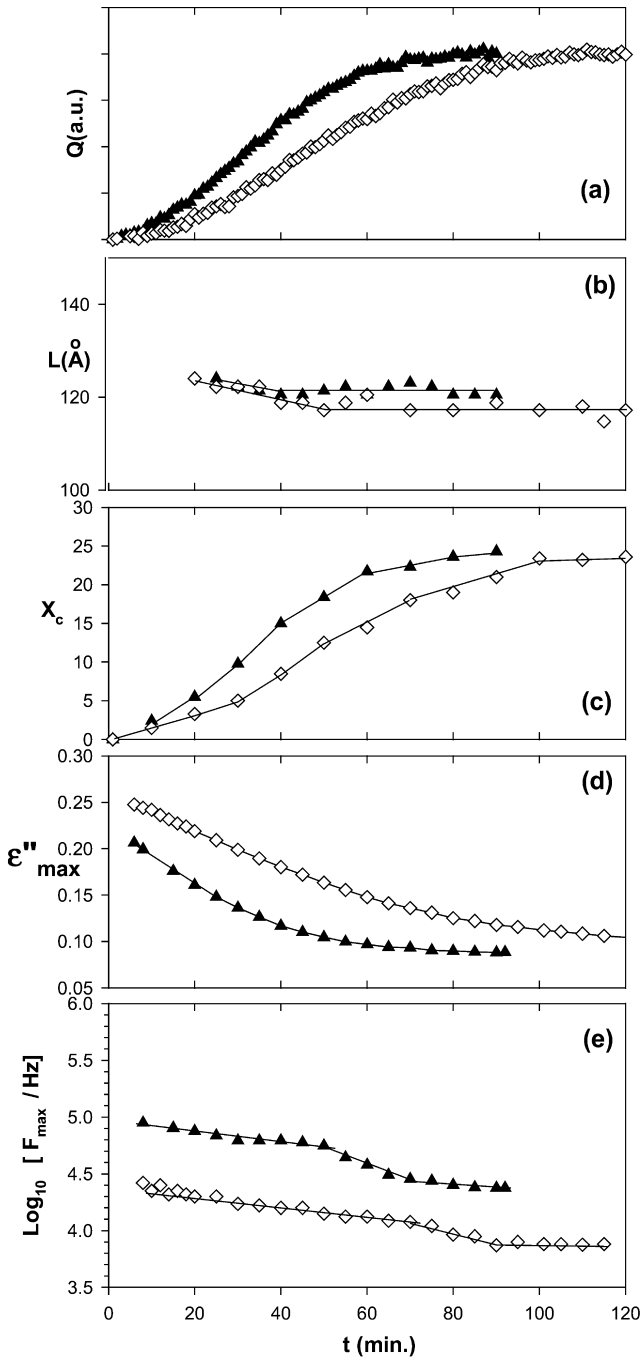

Fig. 2. Summary of physical parameters obtained from the SWD experiment for PEN: 152 °C (◇), 157 °C (▲). (a) SAXS integrated intensity Q. (b) Long spacing L, (c) WAXS Crystallinity X_c, (d) ε''_{max} and (e) F_{max} as a function of crystallization time for two crystallization temperatures.

scattering vector $q = (4\pi/\lambda)\sin\theta$, 2θ being the scattering angle. The time interval between the consecutive patterns is 10 min. The ε'' data from DS are presented as a function of frequency ($F = \omega/(2\pi)$, ω being the angular frequency).

The initial amorphous state is characterised by a broad halo in the WAXS diagram, by a continuous scattering decreasing with the q-vector in the SAXS pattern, which is due to the liquid-like state, and by the presence of a relaxation process characterised as a maximum in ε'' centred around a F_{max} value of $\simeq 2 \times 10^4$ Hz in the DS data. The observed relaxation can be identified with the α-process of PEN [8]. The α-relaxation appears as a consequence of the segmental motions of the amorphous phase above the glass transition temperature. As the time increases, the onset of crystallization is manifested by the incipient appearance of Bragg peaks in the WAXS patterns characterising respectively the [010], [100] and [−110] reflections of the triclinic unit cell of the PEN crystalline phase [11]. In the SAXS pattern, an increase of the scattering at lower q-values is observed that develops into a well-defined peak centred at $q = 0.051$ Å^{-1} corresponding to a long spacing L of ca. 123 Å. The earlier mentioned structural features are accompanied by changes in the dynamics of the amorphous phase as revealed by the simultaneous DS experiment. There, the α-relaxation exhibits an intensity decrease and a shift towards lower values of F_{max} as the crystallization time increases. A visualization of the changes in the aforementioned characteristic parameters simultaneously measured for two different crystallization temperatures is presented in Fig. 2. In Fig. 2 we have represented as a function of the crystallization time: (a) the Lorentz corrected integrated SAXS intensity (Q) (in arbitrary units), (b) the long period values (L) calculated from the Lorenz corrected SAXS intensity through $L = 2\pi/q_{max}$, (c) the values for the weight fraction index of crystallinity (X_c) calculated according to the method of Blundell and Osborn [15], (d) the maximum of the dielectric loss (ε''_{max}) and (e) the frequency of maximum loss, F_{max}.

As far as the X-ray scattering data are concerned, it is seen that for times below a characteristic one (about 80 min for $T = 152$ °C, and 60 min for $T = 157$ °C) X_c and Q continuously increase while L remains relatively constant. This behaviour is characteristic for a primary crystallization process. At longer times, X_c and Q attain constant values. The latter behaviour is characteristic of a secondary crystallization process.

In relation to the dielectric experiments, Fig. 2(d) shows that the intensity of the α relaxation, ε''_{max}, continuously decreases with crystallization time and subsequently tends to level off similarly as observed for X_c and Q. However, the frequency of maximum loss, F_{max}, suffers a characteristic discontinuous decrease only around the cross-over time marking the transition from primary to secondary crystallization.

4. Discussion

From the simultaneous SWD-experiments the following relationship between structure and dynamics can be inferred. For times shorter than a characteristic one, the initial strong reduction of the mobile material, reflected by the decrease of ε''_{max}, parallels the increase of crystallinity and integrated intensity Q. It must be noted that although

ε''_{max} does not give the relaxation strength, which is related to the total amount of relaxing material [5], a reasonable experimental correlation of both magnitudes has been shown to exist [8]. During the primary crystallization, the remaining mobile material only slightly change the average segmental mobility in the amorphous phase as reflected by the moderate variation observed in F_{max}. Around the characteristic time when primary crystallization is nearly completed, F_{max} exhibits a notable discontinuous decrease indicating an onset of restrictions in the dynamics of the remaining mobile fraction. The three earlier mentioned features which emerge directly from the simultaneous SAXS, WAXS and DS experiments enable us to propose the following explanation for the cold crystallization of PEN in the investigated temperature range. During the primary crystallization, a nanostructure of lamellar stacks develops as detected by the incipient appearance of a long spacing. In accordance with previous structural models [16], this nanostructure induces the existence of an amorphous phase located within the lamellar stack between consecutive crystalline lamellae and another located in the inter-lamellar stack volume. Although the amount of lamellar stacks increases with time, as revealed by the increase observed in both X_c and Q and the decrease of ε'', the average distance between the gravity centres of consecutive lamellae within the stacks does not significantly change as revealed by the slight variation of the long spacing. In this regime the average mobility of the remaining mobile amorphous phase is slightly affected, as revealed by the small variation with time of F_{max}. Moreover, the invariance of the long spacing and the concurrent discontinuous decrease of F_{max} upon passing through the time marking the transition from primary to secondary crystallization, suggest that the restriction of the mobility mainly affects the amorphous phase located in the inter-lamellar stacks and not the amorphous phase located within the lamellar stacks. We propose that the amorphous regions located between consecutive crystals within the lamellar stack become strongly restricted in its average mobility as soon as the lamellar stack is formed during primary crystallization. This would contribute to the observed change in the shape of the dielectric relaxation during primary crystallization but not to significant changes of F_{max} which mainly would predominantly originate in the inter-lamellar stacks amorphous regions. A similar model was recently proposed to explain crystallization experiments in PET [9] and poly(ether ether ketone) (PEEK) [17] and oxygen transport properties of PET [18]. In fact, the mentioned oxygen permeation measurements indicate that the amorphous region within the lamellar stacks can be associated with the rigid amorphous phase (RAF) [19]. It is to be noted that an irregular insertion of small secondary crystals between consecutive lamellar crystals will certainly tend to reduce mobility without producing significant changes in the long period peak [20]. However, on the basis of the above discussion the low mobility expected for the intra-lamellar amorphous phase would tend to prevent the insertion mechanism. It is only at the end of primary crystallization that a discontinuous reduction in the mobility of the amorphous phase is detected suggesting that initial secondary crystals may act as physical cross-links in the amorphous phase slowing-down its dynamics. Although a qualitatively similar behaviour has been also observed during the cold crystallization of PET [9] some slight differences must be noticed. In PET, similar experiments have shown stronger discontinuities in the behaviour of F_{max} versus crystallization time. In contrast to PET, which under common crystallization conditions exhibits a spherulitic morphology [21], PEN develops, upon cold crystallization, dendritic-like semicrystalline structures [12]. In particular, thorough analysis of SAXS experiments has shown that in PEN the cold crystallization process proceeds through sparse volume filling during primary crystallization [16]. In this case, the separation between primary and secondary crystallization can be not so well defined as for an essentially spherulitic system because impingement of lamellar stacks may occur locally during primary crystallization. This peculiar crystallization behaviour of PEN may be responsible for the less discontinuous behaviour followed by F_{max} during crystallization as compared to the more discontinuous one found in PET. Moreover, as proposed by Schultz et al [22], 'loose' spherulites may first form and become more densely loaded with secondary lamella stacks in later stages of primary crystallization before complete spherulitic impingement. Such a possibility has been supported by investigations involving simultaneous measurements of wide-and small-angle X-ray scattering during isothermal crystallization of PET [23] and PEEK [24]. In both cases, secondary lamellae appearing before spherulitic impingement may restrict amorphous phase dynamics or even inducing the appearance of low frequency shoulders in the α-relaxation process as observed in PET crystallised close to T_g [25].

5. Conclusions

In summary, the main features which are directly derived from our simultaneous SAXS, WAXS and DS experiments support a view for cold crystallization in PEN characterised by the following features. During primary crystallization, a nanostructure of lamellar stacks develops as detected by the appearance of a long spacing. Although the amount of lamellar stacks increases with time, as revealed by the increase observed in both X_c and Q and the decrease of ε''_{max}, the average distance between the gravity centres of consecutive lamellae within the stacks does not significantly change as revealed by the constancy of the long spacing. In this regime the average mobility of the remaining amorphous phase is slightly affected, as revealed by the slight change of F_{max}. The invariance of the long spacing as well as the observed discontinuous decrease in F_{max} upon

passing from primary to secondary crystallization suggests that the restriction of the amorphous phase mobility mainly occurs in the inter-lamellar stacks regions and not in the intra-lamellar stacks amorphous regions.

Acknowledgements

The authors are indebted to MCYT (grant FPA2001-2139) Spain, for generous support of this investigation. The experiments at HASYLAB (Hamburg, Germany) have been funded by the IHP-Contract HPRI-CT-1999-00040 of the European Commission (EC(ERBFMGEDT 950059) and II-00-015 EC). C.A. thanks the Comunidad de Madrid (Spain) for the tenure of a post-doctoral fellowship.

References

[1] Baltá-Calleja FJ, Vonk CG. X-ray Scattering of Synthetic Polymers. Amsterdam: Elsevier; 1989.
[2] Stribeck N. J Appl Cryst 2001;34:496.
[3] Wutz C, Bark M, Cronauer J, Döhrmann R, Zachmann HG. Rev Sci Instrum 1995;66:1303.
[4] Eckstein E, Qian J, Thurn-Albrecht T, Steffen W, Fischer EW. J Chem Phys 2000;113:4751.
[5] Williams G. Adv Polym Sci 1979;33:59.
[6] Ezquerra TA, Majszczyk J, Baltá-Calleja FJ, López-Cabarcos E, Gardner KH, Hsiao BS. Phys Rev B 1994;50:6023.
[7] Ezquerra TA, Baltá-Calleja FJ, Zachmann HG. Polymer 1994;35:2601.
[8] Nogales A, Denchev Z, Šics I, Ezquerra TA. Macromolecules 2000;33:9367.
[9] Ezquerra TA, Šics I, Nogales A, Denchev Z, Baltá-Calleja FJ. Europhys Lett 2002;59:417.
[10] Šics I, Ezquerra TA, Nogales A, Baltá-Calleja FJ, Kalnins M, Tupureina V. Biomacromolecules 2001;2:581.
[11] Buchner S, Wiswe D, Zachmann HG. Polymer 1989;30:480.
[12] Baltá-Calleja FJ, Rueda DR, Michler GH, Naumann I. J Macromol Sci—Phys B 1998;37:411.
[13] Stewart ME, Cox AJ, Naylor DM. Polymer 1993;34:4060.
[14] Šics I, Nogales A, Ezquerra TA, Denchev Z, Baltá-Calleja FJ, Meyer A, Döhrmann R. Rev Sci Instrum 2000;71:1733.
[15] Blundell DJ, Osborn BN. Polymer 1983;24:953.
[16] García-Gutiérrez MC, Rueda DR, Baltá-Calleja FJ. J Mater Sci 2001;36:5739.
[17] Nogales A, Ezquerra TA, Denchev Z, Šics I, Baltá-Calleja FJ, Hsiao B. J Chem Phys 2001;115:3804.
[18] Lin J, Shenogin S, Nazarenko S. Polymer 2002;43:4733.
[19] Cheng SZD, Cao M-Y, Wunderlich B. Macromolecules 1986;267:963.
[20] Stribeck N, Bayer R, von Krosigk G, Gehrke R. Polymer 2002;43:3779.
[21] Zachmann HG, Stuart A. Makromol Chem 1960;41:131.
[22] Schultz JM. Makromol Chem Makromol Symp 1988;15:339.
[23] Zachmann HG, Wutz C. In: Dosiëre M, editor. Crystallization of Polymers. Amsterdam: Kluwer; 1993.
[24] Verma RK, Marand H, Hsiao BS. Macromolecules 1996;29:7767.
[25] Fukao K, Miyamoto Y. Phys Rev Lett 1997;79:4613.